Special Series

Coumarin and Carbazole Fluorescently Modified Cellulose Nanocrystals Using a One-Step Esterification Procedure†

Elena Sîrbu,[1] Samuel Eyley,[2*] Wim Thielemans[2*]

[1]*School of Chemistry, University of Nottingham, University Park, Nottingham, NG7 2RD, UK*

[2]*Renewable Materials and Nanotechnology Research Group, Department of Chemical Engineering, KU Leuven, Campus Kulak Kortrijk, Etienne Sabbelaan 53, 8500 Kortrijk, Belgium*

*Samuel.Eyley@kuleuven.be

*Wim.Thielemans@kuleuven.be

†This article has been accepted for publication and undergone full peer review but has not been through the copyediting, typesetting, pagination and proofreading process, which may lead to differences between this version and the Version of Record. Please cite this article as doi: [10.1002/cjce.22624]

Additional Supporting Information may be found in the online version of this article.

Received 17 April 2016; Revised 8 June 2016; Accepted 16 June 2016
The Canadian Journal of Chemical Engineering

DOI 10.1002/cjce.22624

Fluorescent cellulose nanocrystals with carbazole and coumarin functionalities were synthesised in a one-step esterification reaction using carbazole-9-yl-acetic acid and coumarin-3-carboxylic acid respectively, using a *p*-toluenesulfonyl chloride/pyridine system. Characterization with elemental analysis, X-ray diffraction, X-ray photoelectron spectroscopy, infrared, absorption and emission spectroscopy, and AFM and TEM imaging confirmed that a high degree of modification could be achieved (up to DS_{surf} = 1.33) while retaining the CNC core crystallinity and nanoparticle dimensions. The present grafting method gives a straightforward way when compared with previously reported fluorescent labelling methodologies and gives an extremely high grafting density while retaining the CNC crystallinity. UV spectroscopy also indicates fluorescence quenching at high grafting densities so that optimal fluorescence does not necessarily mean maximum grafting density.

Keywords: Pulp and paper, Wood science and engineering, Surface and interfacial chemistry, Materials science and technology

This article is protected by copyright. All rights reserved

INTRODUCTION

Cellulose nanocrystals (CNC) are long rigid spindle-like particles produced by acid hydrolysis of native cellulose.[1] They have attracted a large amount of attention due to their unique properties such as renewability, naturally abundance, biodegradability, excellent mechanical properties and low environmental impact.[2–6] They have been widely studied as a reinforcing agent in a wide range of polymer matrices.[7–9] Beside this initial application, the potential of CNCs to be used as a building block in more complex systems has been recognised and they have since been investigated for applications ranging from optical materials,[10,11] to permselective membranes,[12] electrode modifiers for electrochemical sensors,[13] supercapacitors,[14–16] and algae flocculants with and without pH responsiveness.[17,18] While many of these applications can make use of "unmodified" cellulose nanocrystals, i.e. as extracted from native cellulose, further expansion of the applications of these excellent materials in advanced materials requires the introduction of additional functionalities through surface modification.[19] One example is the introduction of fluorescence, the subject of this paper.

Fluorescent polymers have become increasingly used as an important macromolecular material in the development of sensors,[20,21] as fluorescent probes in chemical sensing,[22,23] or for bio–imaging and labelling in nanomedicine.[24] Karakawa et al. reported on the memory effect of carbazole-substituted cellulose under homogeneous reaction conditions, the first report on this characteristic for cellulose-based polymers.[25] Zhang et al. have homogeneously synthesised carbazole-substituted hydroxyethyl cellulose (HEC) where, by increasing the cellulose degree of substitution with carbazole, the fluorescence lifetime was increased.[26] The

fluorescent intensity of carbazole-substituted hydroxyethyl cellulose was also found to be stronger than for the carbazole derivative itself. At the same time, coumarin derivatives are important fluorescent dyes with high photoluminescence quantum efficiencies, and uses in optoelectronic materials, while they also display anti-tumoral, anti-coagulant, and anti-oxidant properties.[27–31]

Fillponen et al. covalently linked an azide-bearing fluorescent molecule in a three step reaction: TEMPO mediated oxidation was followed by propargylamine grafting by carbodiimide-mediated amide coupling followed by a Copper(I)–catalysed Azide-Alkyne Cycloaddition reaction (i.e. azide-alkyne click reaction) with azido-coumarin and azido-anthracene. This procedure resulted in fluorescent compounds but only with a 0.1 degree of substitution at the surface.[32] Another modification with responsive fluorophores involving coumarin derivatives (7-hydrozino-4-methylcoumarin and 7-amino-4-methylcoumarin) was reported by Huang et al. and characterised by spectroscopic and imaging techniques.[33] The grafting consisted in the modification of the anhydroglucose units accessible at the reducing end of the nanocrystals that are in hemiacetal form and which are able to react with amine or hydrazine groups. Due to the low amount of reactive sites, the resulting degree of substitution was also low. Another very recent paper reported on the design of light-responsive mechanically adaptive nanocomposites based on CNC that were modified with 7-coumaryl-(6-isocyanothohexyl) carbamate, but the authors did not report the extent of nanocellulose modification.[34] This specific work used the property of coumarin derivatives to undergo photo-dimerization to form a cyclobutane ring through cycloaddition upon UV light irradiation at a wavelength > 300 nm while the corresponding reverse reaction occurs at a wavelength < 280 nm.

In this paper, we describe a more straightforward approach to modify cellulose nanocrystals with the fluorescent molecules coumarin and carbazole that also allows much higher degrees of substitutions than have been published up to now.

EXPERIMENTAL

Materials

Cotton wool together with Analytical Reagent Grade dichloromethane (DCM), ethanol (EtOH), *N*,*N*-Dimethylformamide (DMF) were purchased from Fisher Scientific. Triethylamine (Et_3N, 99+ %), 1-methylimidazole (99 %), and coumarin-3-carboxylic acid (99 %) were purchased from Sigma Aldrich. Extra dry 99.8 % DMF, extra dry pyridine kept over molecular sieve (99.5 %), bromoacetic acid (99 %), bromoacetyl bromide (98+ %), orange II sodium salt (90 % pure dye content), and carbazole (96 %) were procured from Acros Organics. 98 % *p*-toluensulfonyl chloride (98 %) (TsCl) was purchased from Alfa Aesar. Cellulose extraction thimbles were purchased from VWR International. All chemicals were used as received.

Characterisation FTIR spectrum were collected on a Nicolet 380 FT-IR spectrometer (ThermoElectron Corp.) using OMNIC software. Samples were run in transmission mode using 1-2 mg of sample in 200 mg of anhydrous KBr pellets. The transmission spectra were recorded over 16 scans between 400 to 4000 cm^{-1} wavenumbers with a resolution of 4 cm^{-1}. Elemental analysis (C, H, N, S) data was collected on a Thermo Flash 2000 elemental analyzer using methionine as a calibration standard with linear calibration. C, H, N, and S contents were reported as mass percentage of the sample. Degree of substitution (DS) was calculated using an iterative procedure whereby the empirical formula of the graft added to cellulose was added to the empirical formula

of the anhydroglucose unit until the average error on C (for coumarin grafts) or N (for carbozole grafts) was minimized.

XPS analysis was carried out on a Kratos AXIS ULTRA with a mono-chromated Al kα X-ray source (1486.6 eV) operated at 10–15 mA emission current and 10-12 kV anode potential on samples in powder form. At least three positions on the sample were analysed. XPS data analysis is carried out using CASAXPS software with Kratos sensitivity factors. The high resolution peaks were fitted using a pseudo-Voigt profile (convolution of Gaussian and Lorentzian profile) corrected with an asymmetric correction accounting for the vibrational modes of cellulose that induce peak broadening as a consequence of photon energy absorbed by vibrational transitions in the bonds connected to the atoms of interest.

X-ray diffraction data was collected on a PANalytical X'Pert Pro multi-purpose diffractometer (MPD) in Bragg-Brentano parafocusing geometry, with Cu Kα (45 kV, 40 mA) radiation, automated divergence and receiving slits (10 mm illuminated length), 10 mm beam mask and a step size of 0.02°. Samples were analyzed on a silicon "zero-background" sample holder. The sample stage was rotated during acquisition to reduce preferred orientation effects in the plane of the stage. Rietveld refinement was carried out using Highscore Plus software with subtraction of instrumental background (collected using an empty sample holder) and fitting of a Chebyshev background to determine amorphous content. The crystallinity index was then determined using the method described by Thygesen et al.,[43] whereby the crystalline and amorphous contributions to the diffraction pattern are determined by integration of the fitted profile. The crystallinity index is then calculated according to the following equation where I_c is the crystalline intensity s is the scattering vector,

and s1 and s0 represent the scattering vector at $2\theta = 10°$ and $2\theta = 40°$:

$$\chi_c = \frac{\int_{s0}^{s1} I_c(s)s^2 ds}{\int_{s0}^{s1} I(s)s^2 ds}$$

AFM measurements were carried out on a Dimension 3100 AFM (Bruker) operated by NanoScope IIIa Controller Digital Instruments in tapping mode. The manipulation of the AFM images was performed using Gwyddion 2.32 software. Samples were prepared by depositing a few drops of a solution of 0.012 g/g (1.2 wt%) suspension of cellulose nanocrystals on 1 cm × 1 cm square freshly cleaved mica. The samples were rinsed with deionized water and dried under Ar flow.

For transmission electron microscopy (TEM), drops of cellulose nanocrystal suspension of 0.00001 g/g (0.001 wt%) were deposited on carbon-coated electron microscope TEM grids (Grid S160H) which were previously cleaned using a Plasma Cleaner, Model 1020. After complete drying, these specimens were negatively stained with 2 % uranyl acetate and observed using a JEOL JEM - 2000FXII Scanning Transmission Electron Microscope at an accelerating voltage of 80 kV.

UV spectra were measured on a PerkinElmer Lambda 25 UV-Vis Spectrometer operated with Lambda 25 software using quartz cell with a path length of 1 cm in the 190 – 700 nm range with 1 nm resolution.

Synthesis of Cellulose Nanocrystals

Cellulose nanocrystals were prepared by acid hydrolysis of cotton wool (51.42 g) for 35 minutes in a 0.64 g/g (64 wt%) aqueous H_2SO_4 solution at 45 °C under continuous stirring. The resulting nanowhiskers suspension was diluted with deionized water and

centrifuged three times at 10 000 rpm at 10 °C for 40 min, followed each time by replacing the supernatant with de-ionized water. Dialysis to neutrality of the nanowhiskers suspension against tap water for 2 days was performed to remove residual free acids. To obtain a homogeneous dispersion of the nanowhiskers in water, the suspension was sonified for 5 minutes at 15 % amplitude, at a maximum temperature of 35 °C using a Branson Sonifier. Then, the dispersion was filtered through a fritted glass filter No. 2 and ion-exchanged with Amberlite resin for 24 h, to replace surface cations with protons. The stable suspension was filtered and sonicated once again at dilute concentration, frozen in liquid nitrogen and freeze-dried on a Heto PowerDry PL600 apparatus. Cellulose nanowhiskers were subsequently purified with EtOH Soxhlet extraction for 3 days to remove adsorbed species left over from the hydrolysis procedure.[35] The nanowhiskers were dried in vacuo and were used as such for surface modification reactions. Found: C, 41.96; H, 6.00 %. Calculated for $(C_6H_{10}O_5)_n$: C, 43.43; H, 6.21 %. $\bar{\nu}_{max}$ (KBr) / cm^{-1} 3345 ν(O–H), 2900 ν(C–H), 1636 δ (H_2O), 1430 δ(C–O–H), 1337 δ(C–O–H), 1317 δ(C–O–H), 1205 ν(C–O–C, glycosidic), 1163 ν(C–O–C, glycosidic, asym.), 1112 ν(C2–OH), 1059 ν(C3–OH), 1033 ν(C6–OH), 708 ω(C-OH), 666 ω(C-OH).

Synthesis of Methyl

2-(9H-carbazol-9-yl) acetate

Carbazole (5.05 g, 30.2 mmol) was stirred with dry K_2CO_3 (11.12 g, 2.66 equiv.) in extra dry 99.8 % DMF (50 mL) under argon (Ar) for 45 min at 50 °C before methyl bromoacetate (8.5 mL, 3 equiv.) was added in aliquots over 3.5 hours. The reaction was then stirred at 50 °C for 14 hours, then quenched using cold water (100 mL) and stirred for another 1 hour on ice. The formed precipitate was filtered in a Buchner

funnel and washed with cold water (200 mL). The product was dried under vacuum yielding a white crystalline powder. ^{1}H NMR (300 MHz, DMSO-d_6) ppm 3.68 (br. s., 3 H) 5.36 (br. s., 2 H) 7.23 (t, *J*=5.70 Hz, 2 H) 7.44 (t, *J*=6.92 Hz, 2 H) 7.55 (d, *J*=6.97 Hz, 2 H) 8.16 (d, *J*=5.46 Hz, 2 H); MS (ESI) m/z (%): 262 (M+Na, 100), 240 (M+H, 41), 180(33), 149(9).EA: Found: C, 74.75; H, 5.48; N, 5.48; Calculated: C, 75.30; H, 5.48; N, 5.85.

Synthesis of carbazole-9-yl-acetic acid

Methyl 9H-carbazole-9-acetate (6 g, 25 mmol) and KOH solution (10 %, 460 mL) were added into a large single-aperture flask and heated to reflux for 5 hours under vigorous stirring. The mixture was cooled down in an ice bath and quenched with cold water (200 mL). The solution was acidified to pH 4-5 with 10 % diluted HCl (~260 mL). The formed precipitate was washed with water and dried under vacuo. The product was a white solid (yield 75 %). ^{1}H NMR (300 MHz, DMSO-d6) d ppm 5.22 (s, 2 H) 7.22 (t, J=7.21 Hz, 2 H) 7.43 (t, J=7.30 Hz, 2 H) 7.55 (d, J=7.91 Hz, 2 H) 8.15 (d, J=7.44 Hz, 2 H) MS (ESI) m/z (%): 248 (M+Na, 100), 226(M+H, 33), 149(20), 116(11). EA: Found: C, 74.51; H, 4.87; N, 5.99. Calculated C, 74.65; H, 4.92; N, 6.22.

Synthesis of carbazole-9-yl-acetate cellulose 1 (Cz-a-CNC1)

Cellulose nanocrystals (500 mg), carbazole-9-yl-acetic acid (450 mg, 2 mmol), and *p*-toluensulfonyl chloride (381 mg, 2 mmol) were suspended in dry pyridine (50 ml) under argon atmosphere and heated at 80 °C for 24 hours. The solid product was filtered from the red suspension through a cellulose Soxhlet extraction thimble followed by the purification of the reaction product by Soxhlet extraction with DCM

for 24 hours and EtOH for 72 hours. The resulting modified nanocrystals were dried in vacuo to give white-cream solid nanoparticles. Found: C, 46.66 %; H, 5.70 %; N, 0.84; S, 0.29%. Calc. for $C_{7.64}H_{11.17}O_{5.17}N_{0.12}S_{0.02}$ (DS(N) = 0.12, DS(OSO3H) = 0.02, 1.85% water): C, 47.91; H 6.09; N, 0.86; S, 0.29 %. $\bar{\nu}_{max}$ (KBr) / cm^{-1} 3345 ν(O−H), 2900 ν(C − H), 1744 ν(C=O), 1627 ν(C=C), 1599 ν(C=C), 1485 ν(arom.), 1456 ν(arom.), 1429 δ(C − O − H), 1358 δ(C − N), 1324 δ(C − N), 1280 ν(C − O − C, glycosidic), 1161 ν(C−O−C, glycosidic, asym.), 1112 ν(C2−OH), 1058 ν(C3−OH), 1034 ν(C6−OH), 753 ω(C-OH), 722 ω(C-OH), 666 ω(C−OH).

Synthesis of carbazole-9-yl-acetate cellulose 2 (Cz-a-CNC2)

Synthesized as described for Cz-a-CNC1 with *p*-toluenesulfonyl chloride (762 mg, 4 mmol) and carbazole-9-yl-acetic acid (900 mg, 4 mmol). Found: C, 51.34 %; H, 5.42%; N, 1.67; S, 0.21 %. Calc. for $C_{9.84}H_{12.74}O_{5.32}N_{0.27}S_{0.02}$ (DS(N) = 0.27, DS(OSO_3H) = 0.02, 1.3 % water): C, 52.92 %; H 5.90 %; N, 1.72; S, 0.21%. $\bar{\nu}_{max}$ (KBr) / cm^{-1} 3345 ν(O−H), 2900 ν(C−H), 1748 ν(C=O), 1627 ν(C=C), 1599 ν(C=C), 1485 ν(arom.), 1456 ν(arom.), 1428 δ(C−O−H), 1356 δ(C−N), 1324 δ(C−N), 1280 ν(C−O−C, glycosidic), 1161 ν(C−O−C, glycosidic, asym.), 1112 ν(C2−OH), 1059 ν(C3−OH), 1034 ν(C6−OH), 751 ω(C-OH), 722 ω(C-OH), 667 ω(C−OH).

Synthesis of carbazole-9-yl-acetate cellulose 3 (Cz-a-CNC3)

Synthesized as described for Cz-a-CNC1 with *p*-toluenesulfonyl chloride (1.14 g, 6 mmol) and carbazole-9-yl-acetic acid (1.35 g, 6 mmol). Found: C, 53.36%; H, 5.43 %; N, 1.86, S, 0.16 %. Calc. for $C_{10.50}H_{13.21}O_{5.36}N_{0.32}S_{0.01}$ (DS(N) = 0.32, DS(OSO_3H) = 0.01, 1.9% water): C, 53.78; H 5.89; N, 1.92; S, 0.16 %. $\bar{\nu}_{max}$ (KBr) / cm^{-1} 3344 ν(O−H), 2900 ν(C−H), 1748 ν(C=O), 1627 ν(C=C), 1599 ν(C=C), 1485 ν(arom.),

1456 ν(arom.), 1428 δ(C−O−H), 1356 δ(C−N), 1324 δ(C−N), 1280 ν(C−O−C, glycosidic), 1161 ν(C−O−C, glycosidic, asym.), 1112 ν(C2−OH), 1059 ν(C3−OH), 1034 ν(C6−OH), 751 ω(C-OH), 722 ω(C-OH), 667 ω(C−OH).

Synthesis of coumarin-3-carboxylate cellulose (Co-c-CNC)

Cellulose nanocrystals (500 mg), coumarin-3-carboxylate (522 mg, 2.75 mmol), and *p*-toluensulfonyl chloride (524 mg, 2.75 mmol) were suspended in dry pyridine (50 mL) under argon atmosphere and heated at 80 °C for 24 hours. The solid product was filtered from suspension through a cellulose Soxhlet extraction thimble followed by the purification of the reaction product by Soxhlet extraction with DCM for 24 hours and EtOH for 72 hours. The resulting modified nanocrystals were dried in vacuo to give white-cream solid nanoparticles. Found: C, 49.73 %; H, 4.84; S, 0.25 %. Calc. for $C_{9.26}H_{11.30}O_{6.03}S_{0.02}$ (DS(coumarin) = 0.33; DS(OSO_3H) = 0.02; 1.9 % water): C, 49.67; H 5.30; S, 0.26 %. $\bar{\nu}_{max}$ (KBr) / cm^{-1} 3345 ν(O−H), 2901 ν(C−H), 1762 ν(C=O), 1609 ν(C=C), 1566 ν (arom.), 1455 ν (arom.) 1428 δ(C−O−H), 1335 δ(C−O−H), 1314 δ(C−O−H), 1246 ν(C–O–C), 1208 ν(C−O−C, glycosidic), 1162 ν(C−O−C, glycosidic, asym.), 1112 ν(C2−OH), 1059 ν(C3−OH), 1033 ν(C6−OH), 795 ω(C-OH), 763 ω(C-OH), 705 ω(C−OH), 666 ω(C−OH).

RESULTS AND DISCUSSION

In this paper, cellulose nanocrystals were prepared by acid hydrolysis of bleached cotton wool using 0.64 g/g (64 wt%) sulfuric acid according to earlier published standard procedures. Adsorbed impurities on the nanocrystal surface left over from the hydrolysis procedure were removed by soxhlet extraction with ethanol for 72 h.[35] After drying, the nanocrystals were surface modified under heterogeneous conditions,

in order to graft two carboxy-terminated fluorescent molecules through ester formation. For this, cellulose nanocrystals were reacted with carbazole-9-yl-acetic acid (produced via the reaction of carbazole with methyl bromoacetate (Scheme 1a)) and coumarin-3-carboxylic acid in a *p*-toluenesulphonyl chloride/pyridine system under an argon atmosphere at 80^{o}C for 16 hours (Scheme 1b). The carbazole-9-yl-acetic acid reaction was carried out with increasing molar ratio of the carbazole-9-yl-acetic acid and TsCl activator 1:0.66:0.66; 1:1.33:1.33; 1:2:2 (CNC-OH:acid:TsCl) while the reaction with coumarin-3-carboxylic acid used the following molar ratio of 1:1.83:1.83 (CNC-OH:TsCl:Py). Pyridine was used in excess as solvent at 50 mL for 500 mg of CNC. Carbazole-9-yl-acetic acid and coumarin-3-carboxylic acid are activated with *p*-toluenesulphonyl chloride through formation of anhydrides, followed by a nucleophilic attack of the cellulose surface hydroxyl groups on the carbonyl carbon to give an ester. This methodology was adapted from Brewster and Ciotti[36] and Heuser et al.[37] and has previously been applied successfully in the synthesis of cationic cellulose nanoparticles.[38] The reaction products were purified by Soxhlet extraction with DCM for 24 hours and with ethanol for a further 72 hours followed by drying in vacuo to give off-white carbazole and coumarin modified cellulose nanocrystals.

Infrared spectra of cellulose nanocrystals and carbazole-9-yl acetate modified cellulose (ESI) revealed the appearance of an increasingly prominent signal at 1744.5, 1748.6, and 1748.7 cm^{-1} respectively, which corresponds to the carbonyl stretching vibrations for carbazole-9-yl-acetate cellulose and is identified at a higher wavenumber when compared with the carbazole-9-yl-acetic acid found at 1719.9 cm^{-1} (ESI). Also, multiple aromatic C=C stretching vibrations at 1627, 1599, 1485, and 1456 cm^{-1} appear after modification suggesting successful grafting giving carbazole-

9-yl-acetate cellulose nanocrystals. The bands at 1356 and 1324 cm^{-1} could be attributed to carbon nitrogen C–N vibrations while the peaks at 751 and 722 cm^{-1} can be attributed to an out–of–plane C–H di–substituted aromatic system as found in two benzene rings fused onto pyrrole.[39] Infrared spectra of cellulose nanocrystals and coumarin modified cellulose (ESI) clearly indicated the presence of the carbonyl stretching vibrations at 1762 cm^{-1} and compared with the unmodified CNC spectra, multiple aromatic C=C stretching vibrations at 1609, 1566, 1485, and 1455 cm^{-1} become visible. The bands at 1242 and 1209 cm^{-1} are attributed to carbon oxygen C–O–C ether stretching vibration bands while the signals present at 795 and 763 cm^{-1} can be attributed to an out-of-plane C–H di–substituted aromatic system as in the case of the benzene ring fraction of the coumarin molecule.

X-ray photoelectron spectroscopy (XPS) was used to identify the chemical environments present at the nanocrystal surface. For carbazole-9-yl-acetate cellulose the wide scan XPS revealed the presence of carbon at 286.5 eV, oxygen at 533 eV and nitrogen at 400 eV, while the wide scan spectra of coumarin-3-carboxylate cellulose confirms the presence of only carbon at 286.5 eV and oxygen 533 eV, which are also found in the unmodified cellulose nanocrystals (Figure 1–6 and ESI).

The XPS carbon high resolution scan of carbazole-9-yl-acetate cellulose confirmed the esterification in all three modifications with more detail, showing an increasing surface area of the O–C=O and a large increase in C=C contributions appearing at 289.21 +/– 0.06 eV and 284.58 +/– 0.04 eV respectively. For the same modifications, the nitrogen environment, absent in the unmodified cellulose, shows a single peak at the expected binding energy of 400.1 eV corresponding to the C–N chemical environment found in carbazole.[40]

The crystallinity of the modified CNC was determined by powder X-ray diffraction (XRD) followed by Rietveld refinement[41] (ESI) based on the most recent cellulose I_β crystal structure published by Nishiyama et al.[42] and applying the same procedure as reported by Thygesen et al.[43] The values of the crystallinity index, χ_c, were calculated to be 0.87 for the unmodified cellulose, 0.73, 0.61, and 0.61 for carbazole modifications (Cz-a-CNC1, Cz-a-CNC2, and Cz-a-CNC3 respectively) and 0.52 for coumarin modification respectively (ESI). This corresponds to a crystallinity drop of 14 %, 26 %, 26 %, and 35 % respectively when compared with the initial cellulose crystallinity before modification (0.84). The crystallinity of the total sample is expected to decrease as the grafts are non-crystalline which will increase the amorphous signal. EA allows us to directly determine the degree of substitution and the mass fraction of amorphous material added to the modified CNCs as a result of grafting, which can then be compared with the cellulose crystallinity reduction in the total sample measured through powder X-ray diffraction. EA results for first carbazole modified cellulose (Cz-a-CNC1) showed 46.66 % C, 5.70 % H, 0.84 % N, and 0.29 % S for the second modification conditions (Cz-a-CNC2) 51.34 % C, 5.42 % H, 1.67 % N, and 0.21 % S and for the third modification conditions (Cz-a-CNC3) 53.36 % C, 5.43 % H, 1.86 % N, and 0.16 % S. These results in a determined degree of substitution (DS) based on nitrogen content of 0.12, 0.27, and 0.32 respectively. Thus, the reaction carried out with the molar excess of 1:2:2 of hydroxyl groups to acid and TsCl gives a maximum surface modification of one primary and one secondary hydroxyl groups per each anhydroglucose unit. The coumarin-3-carboxylate cellulose grafting carried out with the molar ratio of 1:1.83:1.83 for CNC-OH:acid:TsCl, present an even higher DS(C) = 0.33 calculated with determined EA mass compositions of 49.73 % C, 4.84 % H.

The calculated mass fractions of amorphous grafts in the modified samples can then be calculated to be 15, 29, and 32 % for carbazole modifications (Cz-a-CNC1, Cz-a-CNC2, and Cz-a-CNC3 respectively) and 29 % for coumarin-3-carboxylate cellulose. The amount of amorphous graft for coumarin-3-carboxylate cellulose (29 %) is slightly lower than the measured reduction in crystallinity between unmodified cellulose and coumarin-3-carboxylate cellulose (35 %). While this may be due to the relatively poor fit of the diffractogram around 25^{o}, the DS of 0.33 for coumarin-3-carboxylate requires a significant amount of modification of the C3-OH. Because this hydroxyl group is instrumental in retaining rigidity in the surface chains, modification of this group may result in a reduction in surface chain rigidity and thus interaction with the underlying crystalline cellulose chains thereby reducing the crystalline signal slightly. Agreement for carbazole modified CNCs is good for lower degrees of substitution where the crystallinity reductions measured by XRD are 14 and 26 % for Cz-a-CNC1 and Cz-a-CNC2 respectively, agreeing rather well with EA determined amorphous graft amounts of 15 and 29 % respectively. For Cz-a-CNC3, XRD determines a reduction in crystallinity of 26 %, while EA shows 32 % amorphous graft amount. This shows that there is certainly no loss of crystallinity upon surface modification (XRD determined crystallinity loss reduction less than chemically determined amorphous graft amount), but could indicate that, despite extensive purification not all N-containing unreacting reagents could be removed from the product.

In line with the retention of the crystallinity of the cellulose nanocrystalline core in the modified samples, the morphology of the carbazole-9-yl-acetate cellulose and coumarin-3-carboxylate cellulose was not affected by the grafting and the rod-like

shape and size of the unmodified cellulose nanocrystals was maintained as can be seen in the AFM (Figure 5) and TEM (Figure 6) images.

As an alternative method to determine the amount of carbazole and coumarin grafted onto the nanocellulose surface, the optical properties of these fluorescently modified CNC were investigated by UV-Vis spectroscopy followed by fluorescence measurements. The latter was also used to confirm that the fluorescence of the grafts was not affected. For this, certain amounts of modified and unmodified cellulose were suspended in a known volume of solvent followed by determination of the absorption spectra (Figure 7 left). The absorbance was compared to standard solutions of the grafted molecules with known concentrations to determine the amount of grafted UV-absorbing grafts. The amounts of fluorescent molecules were thus determined to be 0.376 mmol/g, 0.426 mmol/g, and 0.576 mmol/g, and 0.755 mmol/g for Cz-a-CNC1, Cz-a-CNC2, Cz-a-CNC3 and coumarin-3-carboxylate cellulose respectively.

The amount of grafted fluorophores is very significant and consists of a large increase when compared with the work of Nielsen et al. [20] which reported grafted amounts of 10.4 μmol/g 5-(and-6)-carboxyfluorescein succinimidyl ester (FAM-SE), 4.7 μmol/g 5-(and-6)-carboxytetramethylrhod-amine succinimidyl ester (TAMRA-SE) and 7.3 μmol/g Oregon Green carboxylic acid, succinimidyl ester OG-SE, or with the work of Dong et al. who grafted 30 μmol/g fluorescein-5‘-isothiocyanate (FITC),[24] or 0.02–0.2 μmol/g 5-(4, 6-dichlorotriazinyl) aminofluorescein (DTAF) achieved by Abitbol et al.[44]

The absorption spectra of the Cz-a-CNC1, Cz-a-CNC2 and Cz-a-CNC3 (Figure 7, left) exhibited three absorption bands at around 294, 327, and 339 nm. The Cz-a-CNC1, Cz-a-CNC2 and Cz-a-CNC3 (Figure 8, top left) displayed an intensive

emission between 335–450 nm with the maxima at λ_{max} = 347 and 362 nm located in the UV spectral range. For the concentration of 0.02 mg/mL, the emission peaks are proportional with the absorption peaks while with increasing concentration, e.g. at 0.08 mg/mL, all the emission spectra display almost the same intensity (Figure 8). The emission spectra for Cz-a-CNC3 were recorded for the excitation wavelengths at 294, 327, and 339 nm and the excitation at λ=295 nm gives more than double the emission intensity found for the other two wavelengths (Figure 9, left).

The absorption spectrum of coumarin-3-carboxylate cellulose nanocrystals (Co-c-CNC) (Figure 7, right) presents two absorption bands at 293 nm and 335 nm. The room-temperature fluorescence emission spectrum of Co-c-CNC (Figure 9, bottom right) was then recorded for these excitation wavelengths. It can be seen that the emission intensity at 335 nm was much higher than that at 293 nm while the emission peak positions were maintained at the same wavelength with an intensive emission in the range of 350–550 nm, with a peak maximum at λ_{max} = 422 nm located in the violet–blue–cyan spectral range. The absorption and emission spectra represent further proof of the successful esterification and retention of the fluorescence capacities of the grafts.

Furthermore, the amount of fluorescent molecules grafted on the cellulose nanocrystals as determined by UV-Vis spectroscopy previously (0.376 mmol/g, 0.426 mmol/g and 0.576 mmol/g for carbazole-9-yl-acetate cellulose and 0.755 mmol/g for coumarin-3-carboxylate cellulose, respectively) were used to calculate the DS_{surf} considering the numbers of moles of modification per gram of product using the equation proposed by Eyley et al.[19] The DS_{surf} is therefore the fraction between the product of the number of accessible hydroxyl groups per AGU at the surface and the

number of moles of modification, and the product between the mass fraction of cellulose and number of moles of hydroxyl group per gram on the surface of cellulose nanocrystals. The calculated DS_{surf} become 0.19, 0.22, and 0.30 for carbazole-9-yl-acetate cellulose and 0.39 for coumarin-3-carboxylate cellulose. These values are significantly lower than those found by elemental analysis. The reduced values for DS_{surf} determined by fluorescence measurement are most likely due to quenching effects. This would indeed cause significant reduction in the absorption properties and therefore a lower amount of apparent modification determined on the surface by fluorescence measurements. This hypothesis is supported by the observation that for a high concentration of modified carbazole-9-yl-acetate cellulose, the emission spectra present the same intensities irrespective of the degree of substitution (Figure 8), and similar effects are seen for dissolved carbazole at higher concentrations.

CONCLUSIONS

In conclusion, we have demonstrated that two new fluorescent cellulose nanocrystals esters were successfully synthesised with a surface degree of substitution that can cover more than one primary and one secondary hydroxyl group and in a one-step reaction. The degree in grafted carbazole was also shown to be easily controlled by the reactant ratios. Quenching at higher grafting densities however can be a problem so that maximum grafting density is not always desirable. The present fluorescent modifications can be further tested for toxicity and bioactivity and compatibility and can present potential applications in related applications such as bioimaging, biosensors and phototherapy.[45]

ACKNOWLEDGMENTS

The authors thank the Engineering and Science Physical Sciences Research Council (ESPRC grant EP/J015687/1) and Research Foundation – Flanders (FWO, grant G.0C60.13N) for funding, as well as the University of Nottingham, Nanotechnology and Nanoscience Centre (NNNC) for XPS, TEM and EA services. ES also thanks to University of Nottingham for a European Union Excellence Research Scholarship.

REFERENCES

1. Y. Habibi, L. A. Lucia, O. J. Rojas, *Chem. Rev.* **2010**, *110*, 3479.

2. D. Klemm, F. Kramer, S. Moritz, T. Lindström, M. Ankerfors, D. Gray, A. Dorris, *Angew. Chemie Internat. Ed.* **2011**, *50*, 5438.

3. R. J. Moon, A. Martini, J. Nairn, J. Simonsen, J. Youngblood, *Chem. Soc. Rev.* **2011**, *40*, 3941.

4. A. Dufrense, *Nanocellulose: From Nature to High Performance Tailored Materials*, 1st edition, De Gruyter, Berlin **2012**.

5. K. Kümmerer, J. Menz, T. Schubert, W. Thielemans, *Chemosphere* **2011**, *82*, 1387.

6. S.J. Eichhorn, A. Dufresne, M. Aranguren, N.E. Marcovich, J.R. Capadona, S.R. Rowan, C. Weder, W. Thielemans, M. Roman, S. Renneckar, W. Gindl, S. Veigel, H. Yano, K. Ab, M. Nogi, A.N. Nakagaito, A. Mangalam, J. Simonsen, A.S. Benight, A. Bismarck, L.A. Berglund, T. Peijs, *J. Mater. Sci.* **2010**, *45*, 1.

7. V. Favier, H. Chanzy, J. Y. Cavaille, *Macromolecules* **1995**, *28*, 6365.

8. M. A. S. Azizi Samir, F. Alloin, J.-Y. Sanchez, N. El Kissi, A. Dufresne, *Macromolecules* **2004**, *37*, 1386.

9. X. Cao, H. Dong, C. M. Li, *Biomacromolecules* **2007**, *8*, 899.

10. J. F. Revol, H. Bradford, J. Giasson, R. H. Marchessault, D. G. Gray, *Internat. J. Biol. Macromol.* **1992**, *14*, 170.

11. J. Pan, W. Hamad, S. K. Straus, *Macromolecules* **2010**, *43*, 3851.

12. W. Thielemans, C. R. Warbey, D. A. Walsh, *Green Chem.* **2009**, *11*, 531.

13. S. Y. Liew, S. Shariki, A. Vuorema, D. A. Walsh, F. Marken, W. Thielemans, "Chapter 5 : Cellulose Nanowhiskers in Electrochemical Applications" in *Functional Materials from Renewable Sources*, F. Liebner, T. Rosenau, Eds., ACS Symposium Series 1107, American Chemical Society, Washington, DC **2012**. p. 75-106.

14. S. Y. Liew, W. Thielemans, D. A. Walsh, *J. Phys. Chem. C* **2010**, *114*, 17926.

15. S. Y. Liew, D. A. Walsh, W. Thielemans, *RSC Adv.* **2013**, *3*, 9158.

16. S. Y. Liew, W. Thielemans, D. A. Walsh, *J. Solid State Electrochem.* **2014**, *18*, 3307.

17. D. Vandamme, S. Eyley, G. Van den Mooter, K. Muylaert, W. Thielemans, *Biores. Technol.* **2015**, *194*, 270.

18. S. Eyley, D. Vandamme, S. Lama, G. Van den Mooter, K. Muylaert, W. Thielemans, *Nanoscale* **2015**, *7*, 14413.

19. S. Eyley, W. Thielemans, *Nanoscale* **2014**, *6*, 7764.

20. L. J. Nielsen, S. Eyley, W. Thielemans, J. W. Aylott, *Chem. Commun.* **2010**, *46*, 8929.

21. L. F. Vieira Ferreira, P. V. Cabral, P. Almeida, A. S. Oliveira, M. J. Reis, A. M. Botelho do Rego, *Macromolecules* **1998**, *31*, 3936.

22. P. Bosch, F. Catalina, T. Corrales, C. Peinado, *Chem. Eur. J.* **2005**, *11*, 4314.

23. L. Basabe-Desmonts, D. N. Reinhoudt, M. Crego-Calama, *Chem. Soc. Rev.* **2007**, *36*, 993.

24. S. Dong, M. Roman, *J. Amer. Chem. Soc.* **2007**, *129*, 13810.

25. M. Karakawa, M. Chikamatsu, Y. Yoshida, R. Azumi, K. Yase, C. Nakamoto, *Macromol. Rapid Commun.* **2007**, *28*, 1479.

26. L. Zhang, J. Zhou, L. Zhang, *Macromol. Chem. Phys.* **2012**, *213*, 57.

27. C. R. Moylan, *J. Phys. Chem.* **1994**, *98*, 13513.

28. Z. F. Geng, Y. C. Lian, *J. Appl. Phys.* **1987**, *62*, 49.

29. G. Jones, M. A. Rahman, *J. Phys. Chem.* **1994**, *98*, 13028.

30. I. Kostova, *Curr. Med. Chem. Anticancer Agents* **2005**, 5, 29.

31. I. Kostova, *Mini Rev. Med. Chem.* **2006**, *6*, 365.

32. I. Filpponen, D. S. Argyropoulos, *Biomacromolecules* **2010**, *11*, 1060.

33. J.-L. Huang, C.-J. Li, D. G. Gray, *ACS Sustain. Chem. Eng.* **2013**, *1*, 1160.

34. M. V. Biyani, C. Weder, E. J. Foster, *Polym. Chem.* **2014**, *5*, 5501.

35. M. Labet, W. Thielemans, *Cellulose* **2011**, *18*, 607.

36. J. H. Brewster, C. J. Ciotti, *J. Amer. Chem. Soc.* **1955**, *77*, 6214.

37. E. Heuser, M. Heath, W. H. Shockley, *J. Amer. Chem. Soc.* **1950**, *72*, 670.

38. L. Jasmani, S. Eyley, R. Wallbridge, W. Thielemans, *Nanoscale* **2013**, *5*, 10207.

39. A. V. Chekunov, I. A. Polyakova, *J. Appl. Spectros.* **1969**, *10*, 523.

40. J. Lahaye, G. Nansé, A. Bagreev, V. Strelko, *Carbon* **1999**, *37*, 585.

41. H. Rietveld, *J. Appl. Crystallogr.* **1969**, *2*, 65.

42. Y. Nishiyama, P. Langan, H. Chanzy, *J. Amer. Chem. Soc.* **2002**, *124*, 9074.

43. A. Thygesen, J. Oddershede, H. Lilholt, A. B. Thomsen, K. Ståhl, *Cellulose* **2005**, *12*, 563.

44. T. Abitbol, A. Palermo, J. M. Moran-Mirabal, E. D. Cranston, *Biomacromolecules* **2013**, *14*, 3278.

45. N. Lin, A. Dufresne, *Eur. Polym. J.* **2014**, *59*, 302.

Scheme 1 Synthesis of (a) carbazole-9-yl-acetic acid and (b) carbazole-9-yl-acetate cellulose nanocrystals and coumarin-3-carboxylate cellulose nanocrystals using the TsCl/Py system.

Figure 1 C1s high resolution spectrum of carbazole-9-yl-acetate Cz-a-CNC1

Figure 2 C1s high resolution spectrum of carbazole-9-yl-acetate Cz-a-CNC2

Figure 3 C1s high resolution spectrum of carbazole-9-yl-acetate Cz-a-CNC3

Figure 4 C1s high resolution scan of coumarin-3-carboxylate cellulose

Figure 5 AFM images of a) unmodified cellulose nanocrystals; b) carbazole-9-yl-acetate cellulose and c) coumarin-3-carboxylate cellulose

Figure 6 TEM micrograph of a) unmodified cellulose nanocrystals; b) carbazole-9-yl-acetate cellulose and c) coumarin-3-carboxylate cellulose (negative staining with uranyl acetate)

Figure 7 UV-Vis spectra of carbazole-9-yl-acetate, left, and coumarin-3-carboxylate cellulose, right.

Figure 8 Emission spectra of the three carbazole-9-yl-acetate cellulose modifications, 0.02 mg/mL, left, and 0.08 mg/mL, right.

Figure 9 Emission spectra of carbazole-9-yl-acetate cellulose 3 for λ=294, 327, and 339 nm (0.01 mg/mL), left, and coumarin-3-carboxylate cellulose for λ=293 and 335 nm (0.2 mg/mL), right.

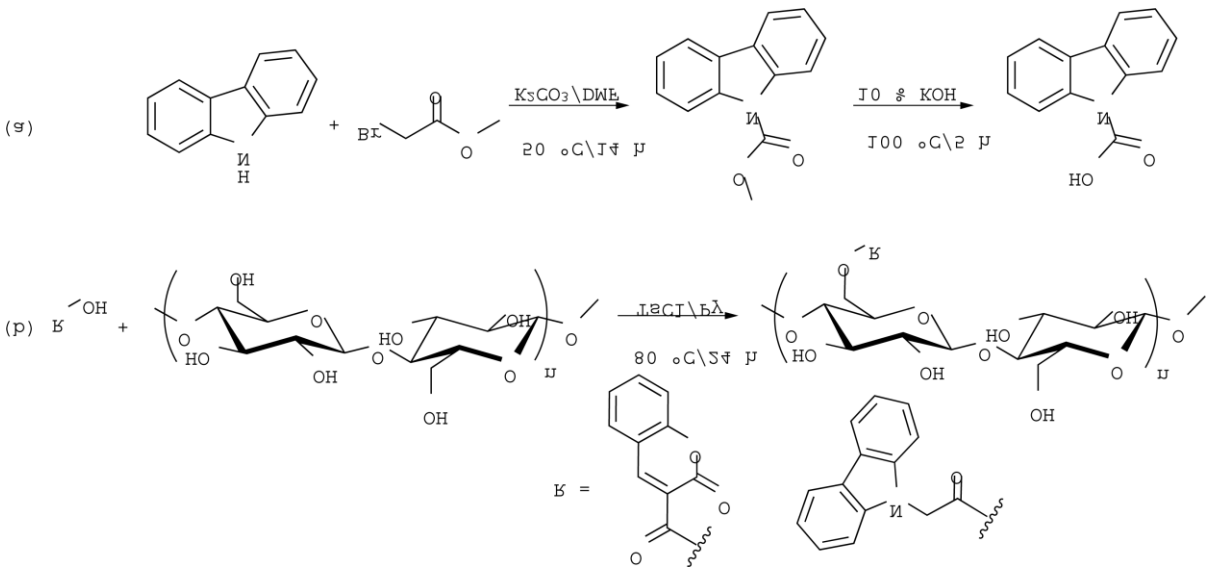

Scheme 1

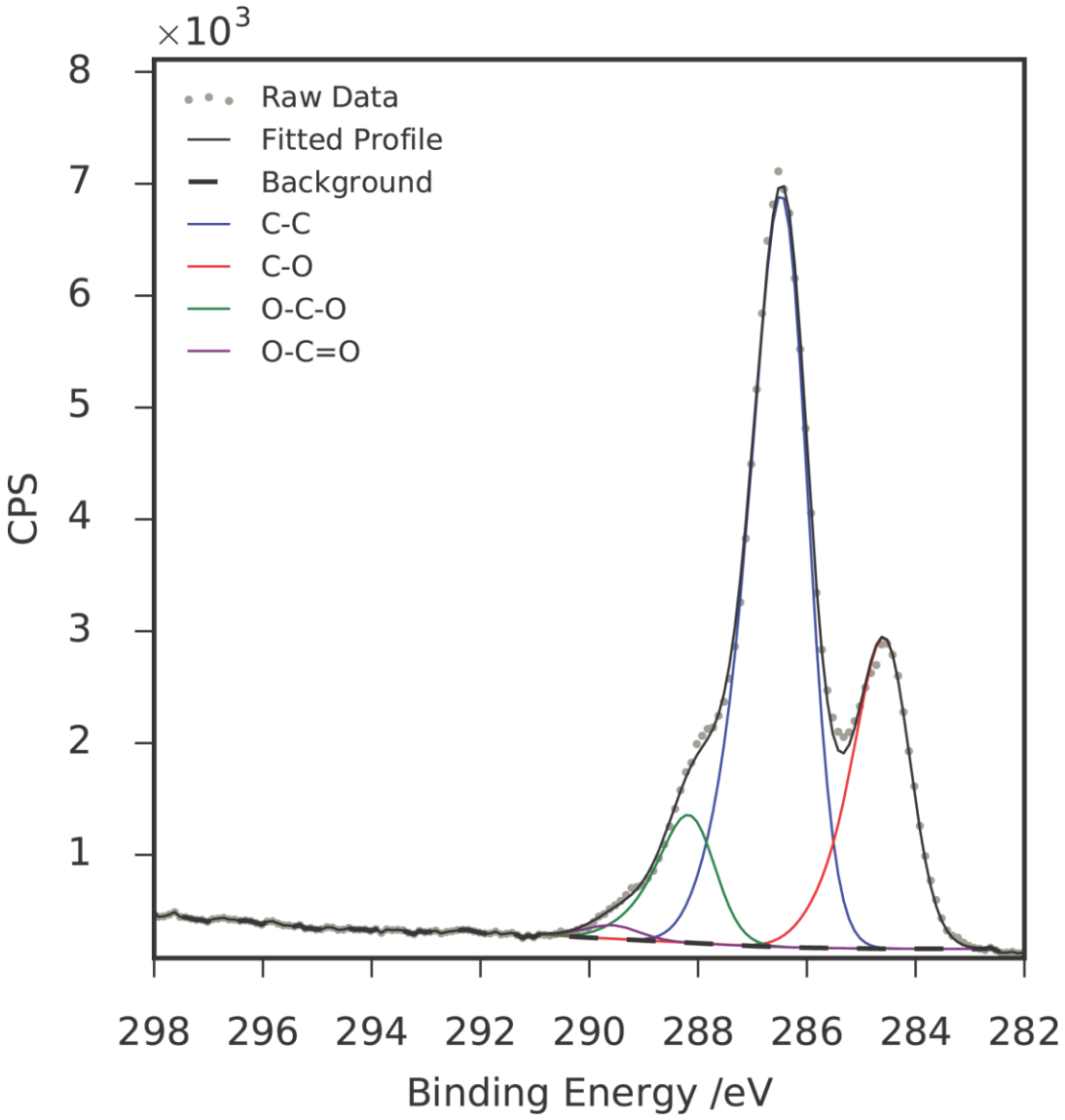

Figure 1

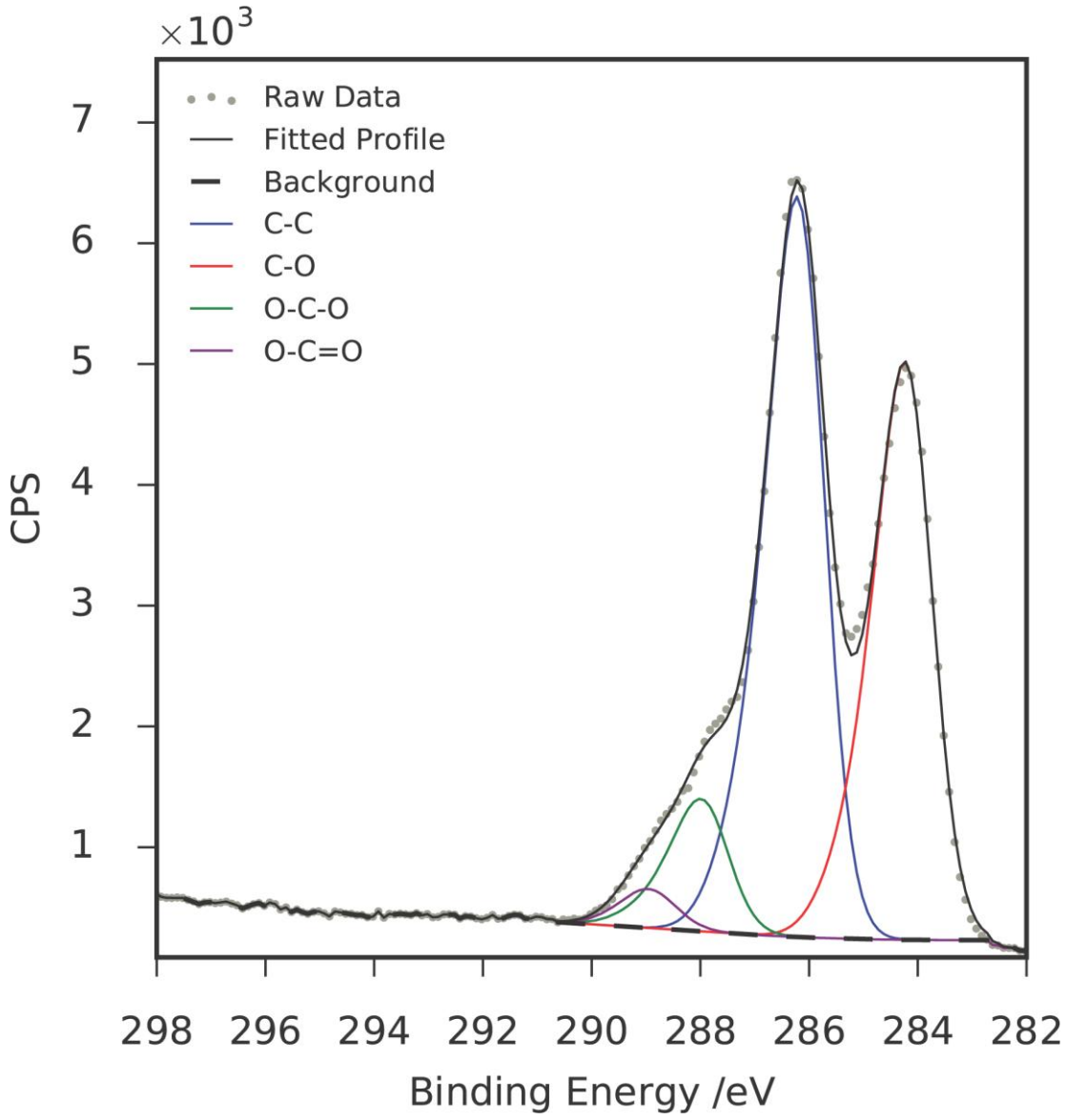

Figure 2

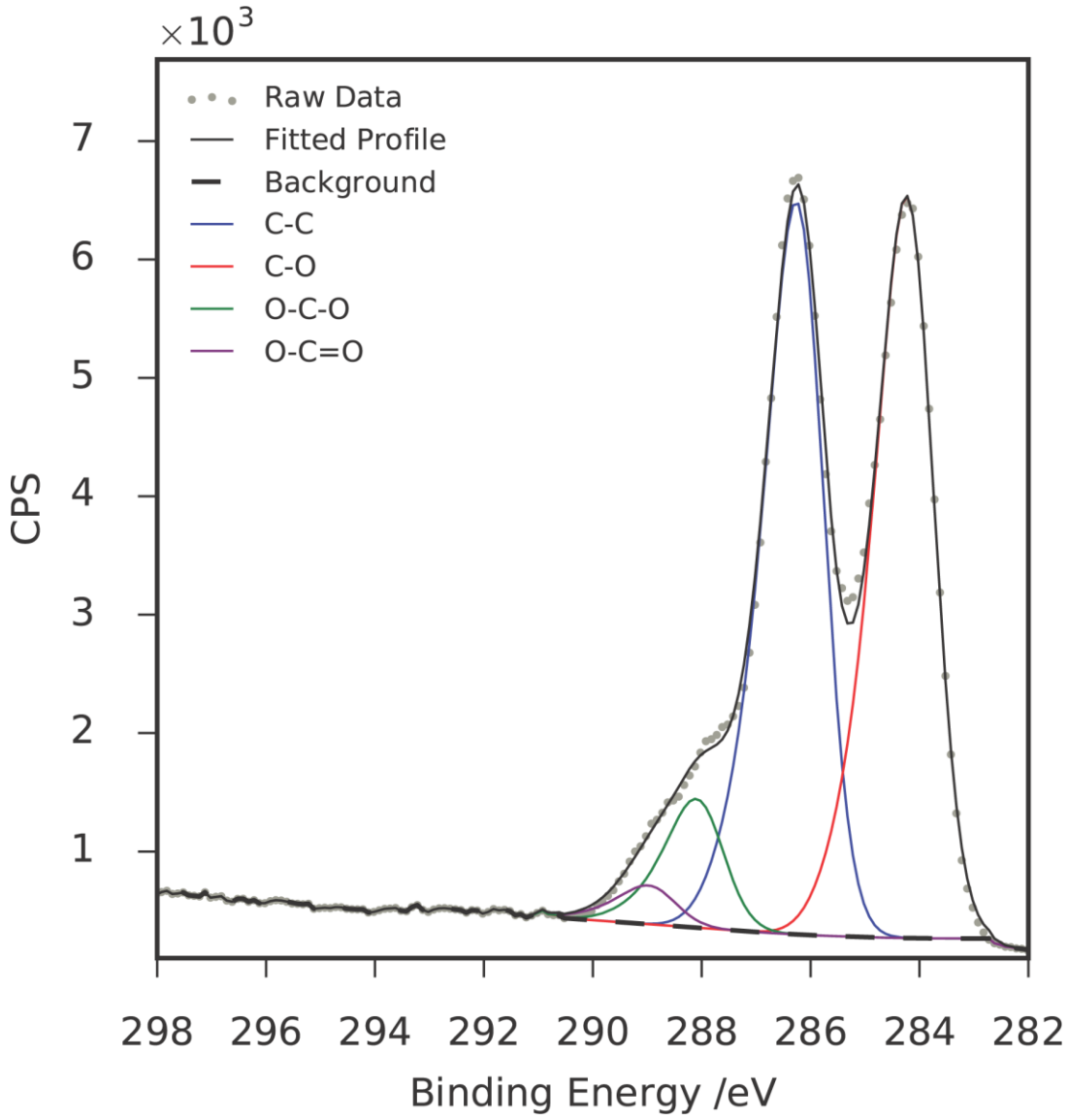

Figure 3

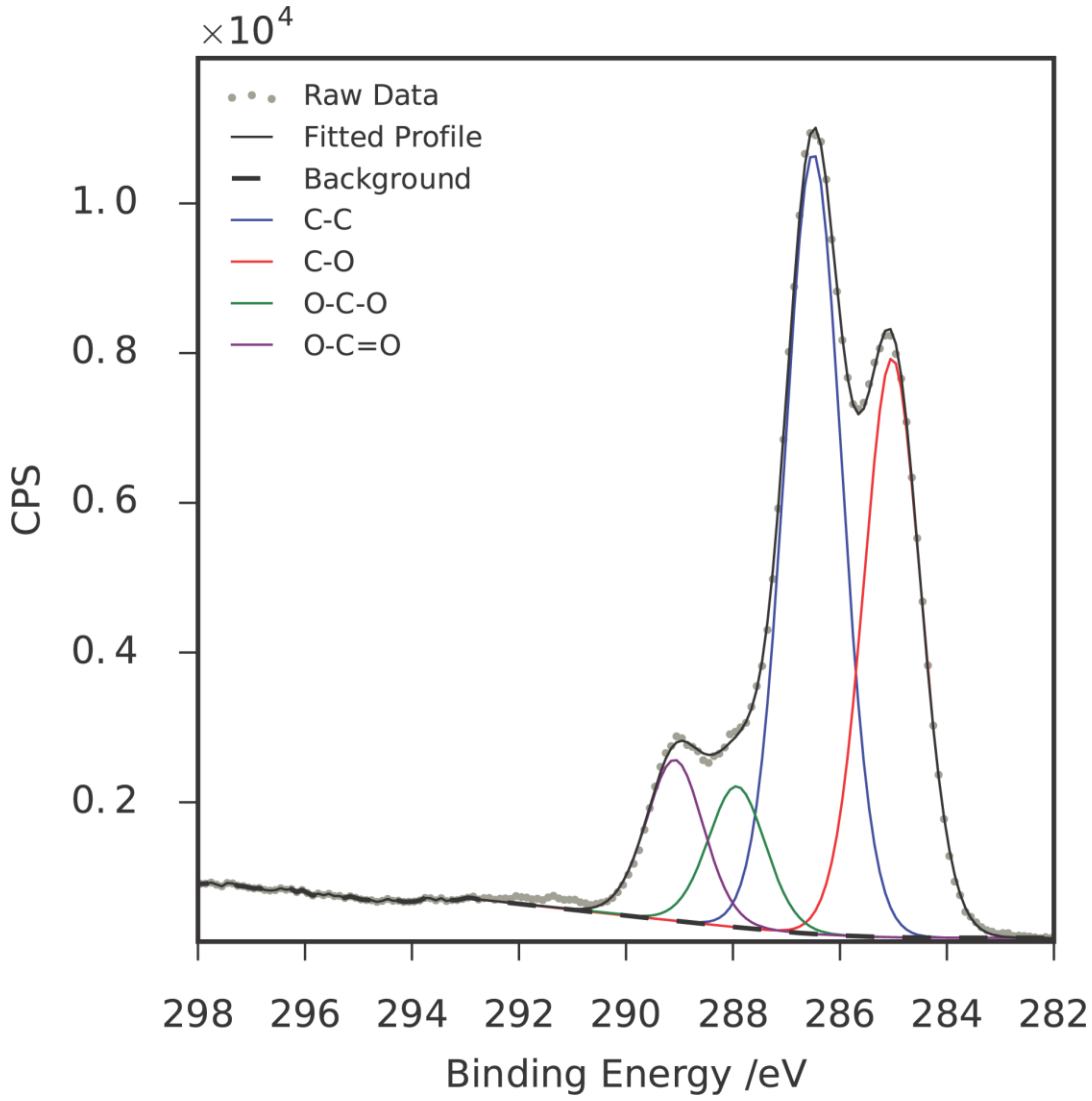

Figure 4

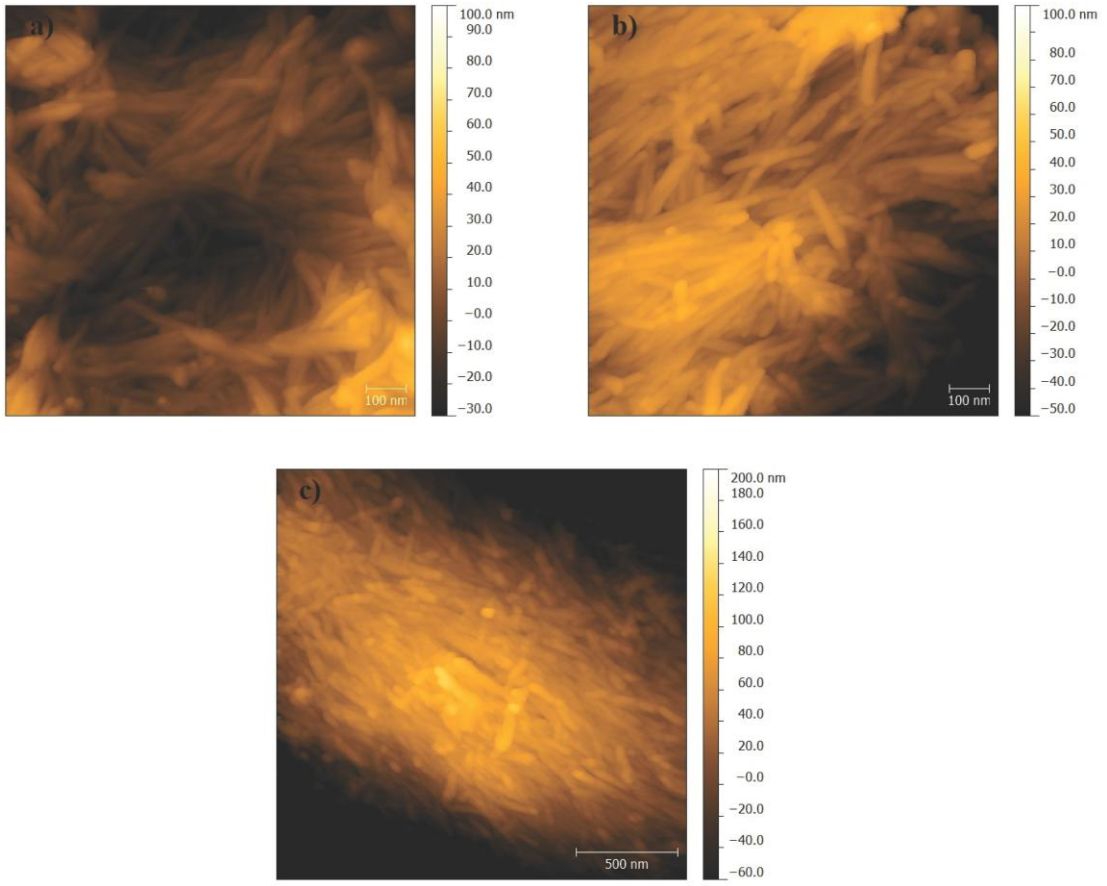

Figure 5

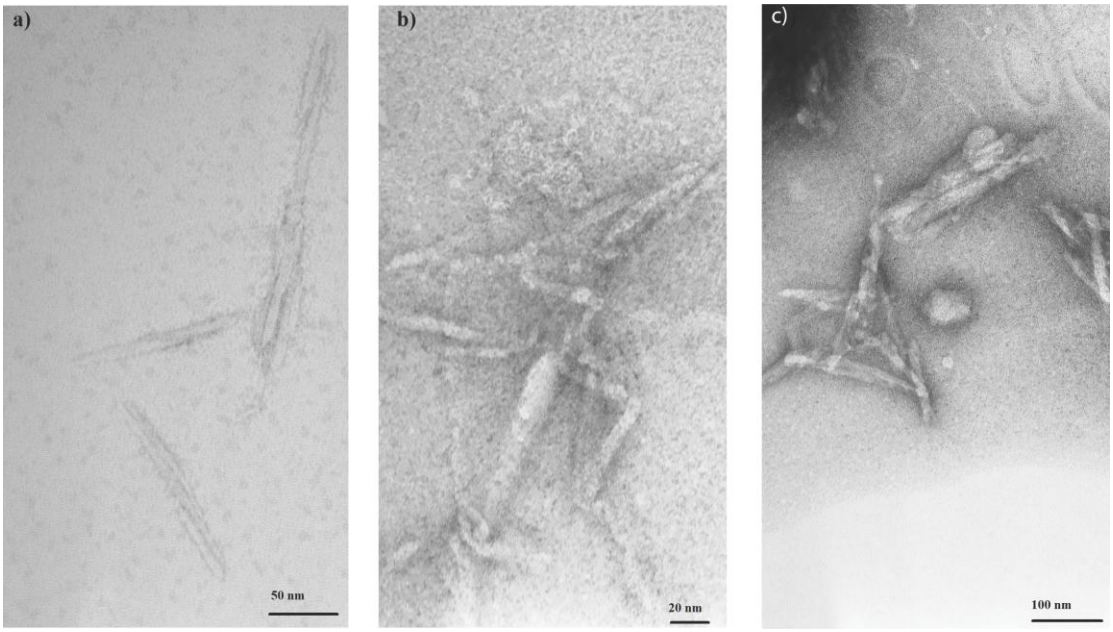

Figure 6

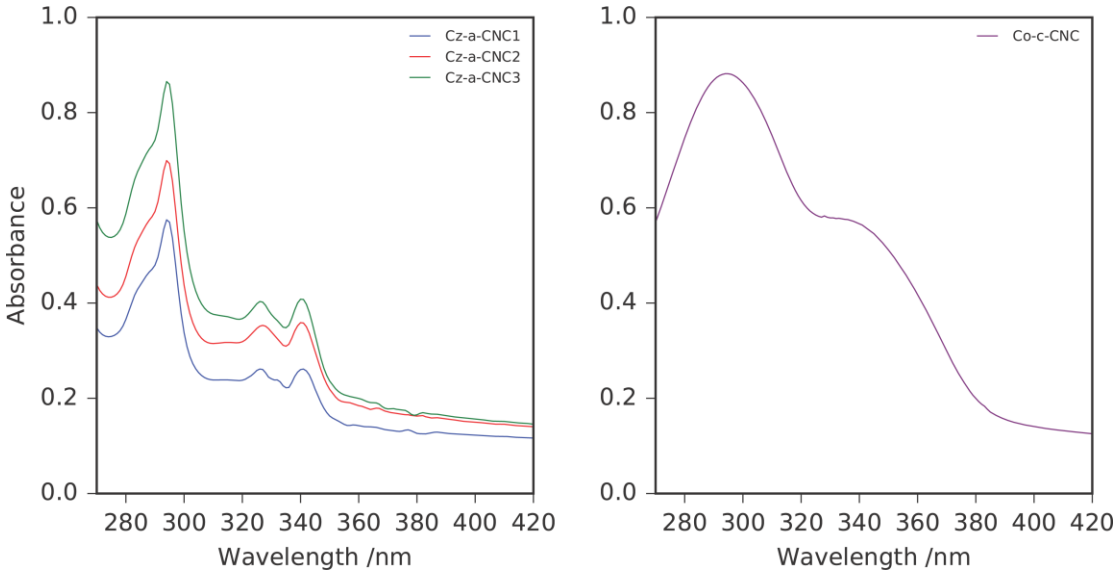

Figure 7

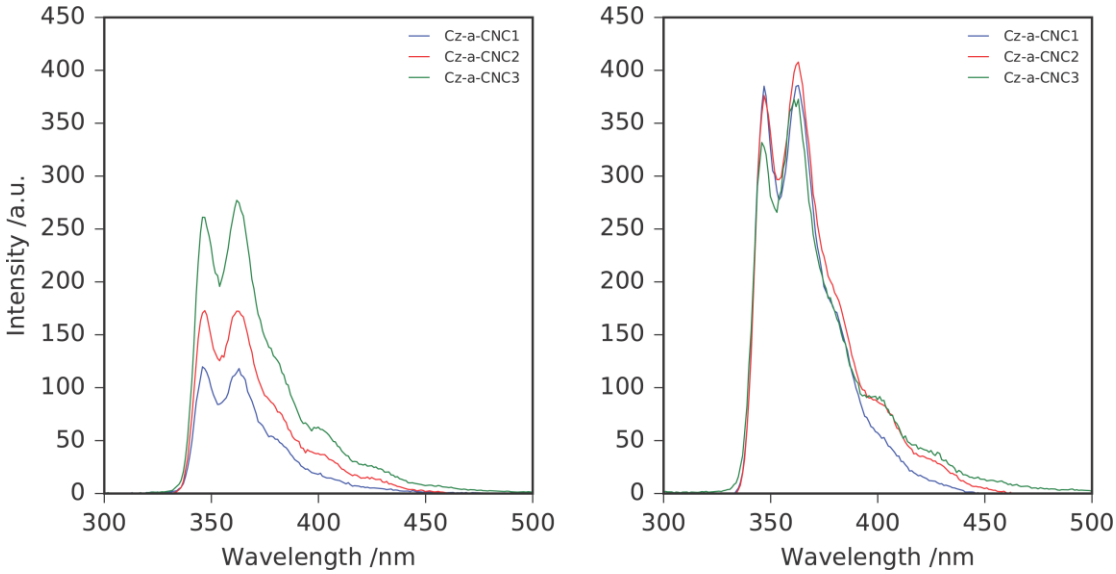

Figure 8

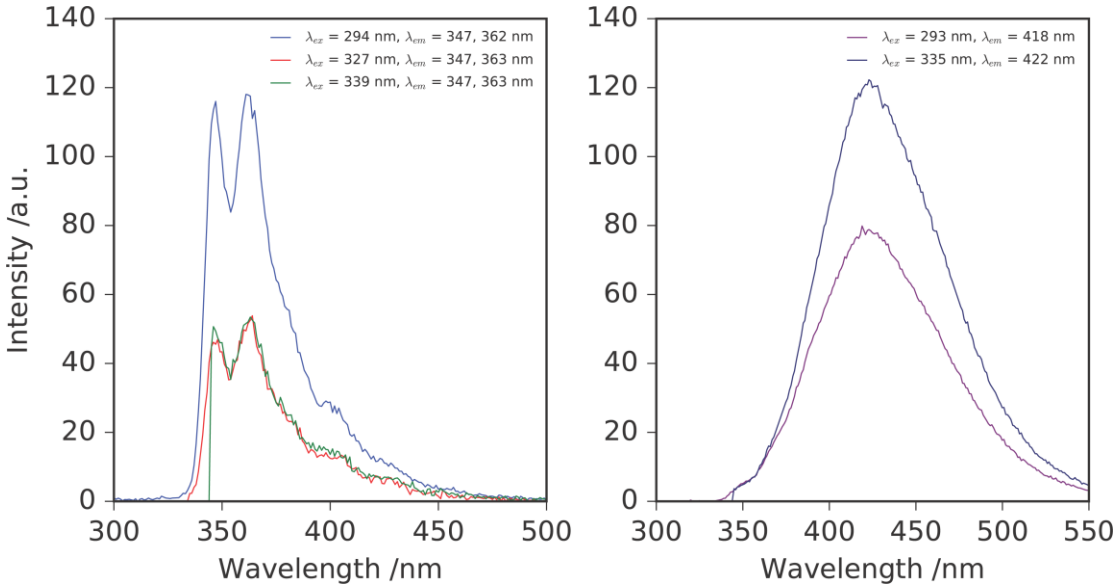

Figure 9